Integrated Arctic Observation System

Research and Innovation Action under EC Horizon2020
Grant Agreement no. 727890

Project coordinator:
Nansen Environmental and Remote Sensing Center, Norway

Deliverable 6.11

Climate model initialization (V2)

Final report on the added value of using data from INTAROS

Start date of project:	01 December 2016	Duration:	63 months
Due date of deliverable:	30 November 2021	Actual submission date:	30 November 2021
Lead beneficiary for preparing the deliverable:	SMHI		
Person-months used to produce deliverable:	31 pm		

Authors: Tim Kruschke (SMHI, lead), Mehdi Pasha Karami (SMHI), Juan C. Acosta Navarro (BSC), Vladimir Lapin (BSC), Pablo Ortega (BSC), Francois Counillon (NERSC), David Gustafsson (SMHI)

Version	DATE	CHANGE RECORDS	LEAD AUTHOR
1.0	16/09/2021	First complete draft	Tim Kruschke
1.1	30/09/2021	Review and draft ready for submission	Kjetil Lygre
1.2	25/11/2021	Extended report as agreed with the Executive Board	Ralf Döscher
1.3	30/11/2021	Review	Helene R.Langehaug
1.4	30/11/2021	Technical review, proof-reading and submission	Kjetil Lygre

Approval	Date:	Sign.
X	30 November 2021	Coordinator

USED PERSON-MONTHS FOR THIS DELIVERABLE (INCLUDING WORK LEADING UP TO THE REPORT)					
No	*Beneficiary*	*PM*	*No*	*Beneficiary*	*PM*
1	NERSC	5	**24**	TDUE	
2	UiB		**25**	GINR	
3	IMR		**48**	UNEXE	
4	MISU		**27**	NIVA	
5	AWI		**28**	CNRS	
6	IOPAN		**29**	U Helsinki	
7	DTU		**30**	GFZ	
8	AU		**31**	ARMINE	
9	GEUS		**32**	IGPAN	
10	FMI		**33**	U SLASKI	
11	UNIS		**34**	BSC	**8**
12	NORDECO		**35**	DNV GL	
13	**SMHI**	**18**	**36**	RIHMI-WDC	
14	USFD		**37**	NIERSC	
15	NUIM		**38**	WHOI	
16	IFREMER		**39**	SIO	
17	MPG		**40**	UAF	
18	EUROGOOS		**41**	U Laval	
19	EUROCEAN		**42**	ONC	
20	UPM		**43**	NMEFC	
21	UB		**44**	RADI	
22	UHAM		**45**	KOPRI	
23	NORCE		**46**	NIPR	
			47	PRIC	

DISSEMINATION LEVEL		
PU	Public, fully open	**X**
CO	Confidential, restricted under conditions set out in Model Grant Agreement	
CI	Classified, information as referred to in Commission Decision 2001/844/EC	

EXECUTIVE SUMMARY

This report describes the final results of the work performed in Task 6.1, which has the main goal of improving the skill of climate predictions, investigating the benefits related to the exploitation of INTAROS data. Such benefits demonstrate a clear potential for users of Arctic data and stakeholders of climate prediction.

A key ingredient to skillful seasonal-to-decadal climate prediction is the use of high-quality observational data, that cover a sufficiently long period, typically at least a few decades to test robustly their impact. This emphasizes the need - from a user perspective - to sustain and continue the production of the various iAOS products.

The works in the task made use of three different datasets produced in INTAROS, namely CERSAT sea-ice concentrations, SMOS sea-thickness, and Arctic-HYCOS river discharges.

The results found in Task 6.1 are:

1. CERSAT sea-ice concentrations were successfully used to assess the skill of SMHI's quasi-operational decadal climate predictions with EC-Earth3 regarding September Northern Hemisphere sea-ice area for a lead time of 11 months (based on the period 1992-2020; correlation of 0.83) and the quality of new assimilation experiments providing potentially better initial conditions for climate predictions (correlation of 0.9 including long-term trend; 0.58 for detrended data, i.e. interannual variability).
2. CERSAT sea-ice concentrations were assimilated for BSC's seasonal climate prediction system employing EC-Earth3. It is shown that the assimilation of sea-ice concentrations does not yield significant benefit for winter seasonal predictions (started on 1 November) but do have a remarkable positive impact on summer seasonal predictions (started on 1 May) regarding the sea-ice edge but also remote North Atlantic SSTs. The latter is shown to be the result of a so-called atmospheric bridge translating the improved sea-ice representation via more realistic large-scale atmospheric variability into the SST-signal.
3. Anomalies derived from sea-ice concentrations as well as SMOS and ENVISAT CCI sea-ice thickness estimates were assimilated in NorCPM, the seasonal-to-decadal climate prediction system developed at NERSC. It is shown that the assimilation of sea-ice concentrations is particularly beneficial for predictions along the sea-ice edge while sea-ice thickness is more important for the central Arctic. Hence, the assimilation of both is complementary and yields the best overall result. Here, the assimilation of SMOS data provides significantly better results compared to ENVISAT CCI.
4. Arctic-HYCOS river discharge is part of the iAOS product, driving from WP2. It has been assimilated to produce a pan-Arctic hydrological analyses and subsequent forecasts with the Arctic-HYPE model. The functionality of this workflow is demonstrated via a use-case addressing the Republic of Sacha (Yakutia), in Far-East Russia, where a sub-set of the Arctic-HYPE model is used for spring flood and river ice breakup forecasting in the major Yakutia rivers.

Table of Contents

1. Introduction

Climate predictions aim to estimate the future evolution of climate on sub-seasonal to decadal time scales. Climate predictability stems from two main sources, external forcing, and the state of the climate system (ocean, atmosphere, land, cryosphere) prior to the forecast initialization. Forecast systems (i.e., initialized climate models) are essential tools in climate prediction and their initialization, which synchronizes the model climate with the real climate, is necessary to exploit the real predictability of the climate system. Knowledge of the climate state at a given point in time is only possible through extensive observations of the different components of the climate system. Furthermore, to correctly evaluate past forecasts and improve the systems, continuous observations in time and space are necessary. A "big picture" view of most of the planet has only been available since satellites became operational in the late 1970s. Additionally, deployment of complementary in-situ observing systems has significantly increased in the past decades, filling important gaps, and as a result improving forecast quality.

The different components of the climate systems interact and have characteristic persistence timescales which together result in predictability. The ocean is the most important component on long timescales (over months to decades), while the atmosphere is critical on short timescales (hours to a week). The land and the sea-ice state in polar regions contain information useful mostly on intermediate timescales (several weeks to over a season). Hence initializing the key variables of the sea-ice component in polar regions may be beneficial for seasonal and decadal predictions not only in polar regions. However, sea-ice initialization is not yet a standard practice in seasonal-to-decadal climate prediction. The partners involved in Task 6.1 of INTAROS perform pioneering research in this context, but correct initialization relies on good observations. sea-ice concentration (SIC) and sea-ice thickness (SIT) are thought to be fundamental variables to initialize sea-ice in fully coupled models. Arctic-wide SIC observations have been available since the late 1970s, while SIT has become available more recently (early 2000s).

Here we report the final findings on the impact of INTAROS Arctic products on seasonal and decadal hindcasts with two contemporary forecast systems, EC-Earth and NorCPM. These rely on the use of novel INTAROS observational datasets for the ocean, sea-ice and land (the specific sets employed are indicated in Sec. 2) either for initialization or evaluation, following the workplan established for Task 6.1. Sec. 3 shows value of using CERSAT sea-ice concentrations (1992-2020) as independent observational reference for evaluating climate model assimilation simulations and quasi-operational decadal predictions. Sec. 4 provides insights into seasonal climate predictions performed after assimilating the very same dataset. Sec. 5 explains the benefits for seasonal-to-decadal predictions after assimilating C2SMOS (SMOS extended by the Cryosat data set, *Wingham et al*., 2006) sea-ice thickness information (2010-2020). In Sec. 6, we present findings of a hydrological use-case where the impact of assimilation of the Arctic-HYCOS hydrological observations (assessed and enhanced within WP2) on monitoring and forecasting of spring flood, river ice breakup and river freshwater flow to the Arctic Ocean is assessed. Sec. 7 summarizes our work, and some future perspectives are drawn in Sec 8.

2. INTAROS data used in this report

Three different products from the INTAROS Data catalog https://catalog-intaros.nersc.no/ have been used for the analyses described in the report (Table 1). These cover different aspects of the ocean, sea-ice and hydrology of the Arctic region. CERSAT sea-ice concentrations were used for evaluating decadal climate predictions and new assimilation experiments (Sec. 3). Additionally, they were assimilated in another set of experiments to generate the initial conditions (ICs) for a seasonal prediction system with EC-Earth (Sect. 4). SMOS and C2SMOS sea-ice thickness has been employed to guide the initialization strategy of a decadal prediction system with EC-Earth and NorCPM (Sect. 3 and 5), and the third product (Arctic-HYCOS river discharges) were assimilated to produce pan-Arctic hydrological analyses and forecast with the Arctic-HYPE model (Sec. 6). Here we refer to C2SMOS as an extension of the SMOS data set with CRYOSAT data.

Table 1. Summary of INTAROS data used in Task 6.1

Product	Variable	Producer	Period covered	Spatial & temporal resolution
SMOS	sea-ice thickness	ESA	2010-2020	~25km; daily
CERSAT	sea-ice concentrations	IFREMER	1992-2021	12.5 km; daily
Arctic-HYCOS	river discharge	SMHI	1979-2020	daily values at 428 river gauging station locations

3. Benefit of new observational sea-ice information for evaluating and initializing climate model simulations for decadal climate predictions (SMHI contribution)

Quasi-operational decadal predictions at SMHI

In D6.1 we presented sensitivity studies assessing the benefit from initializing decadal predictions making use of actual information on sea-ice concentration and thickness.

For that purpose, SMHI developed a method to directly account for sea-ice thickness as represented in ocean reanalysis products and set up a decadal climate prediction system employing this approach in close collaboration with colleagues at the Danish Meteorological Institute (DMI; a synergy with the ARCPATH-project, funded by the Joint Nordic Initiative on Arctic Research). The (atmosphere-ocean) general circulation model (AOGCM) in use is EC-Earth (v3.3.1.1; *Döscher et al.,* 2021), incorporating model components for the atmosphere (IFS c36r4), the ocean (NEMO3.6), and sea-ice (LIM3). A special feature of LIM3 is that it is based on multiple sea-ice categories (five in our case) for a single grid cell of the model. Our initialization method for sea-ice is based on the following procedure: (i) calculating the observed anomaly of local sea-ice volume (SIV; product of sea-ice thickness and concentration)

for a given grid-cell; (ii) distributing these SIV-anomalies into sub-grid contributions of the five categories to the total grid-cell anomaly of sea-ice concentration and thickness. The distribution from (single-category) observed values to five-category contributions is done based on a local non-linear weight-likelihood function that was derived from a multi-centennial control simulation with EC-Earth3 (Tian et al. 2021).

The "observational" data used for initializing ocean and sea-ice fields is taken from ECMWF's ORAS5 ocean reanalysis. For all fields and systems an anomaly initialization approach is used, that means the observational anomalies (compared to the climatological period 1979-2014) are added to the model's climatology. This approach usually prevents substantial initialization shocks and subsequent model drifts. Atmospheric fields have been initialized from ECMWF reanalysis data.

Based on the results of the sensitivity studies presented in D6.1, a quasi-operational decadal prediction system was set up together with DMI, without the data sets listed in Table 1) consisting of 15 ensemble members in total and initialized annually on 1 November throughout the period 1960-2019. This decadal prediction system is participating in the international exchange of annual-to-decadal climate predictions led and coordinated by the UK MetOffice (https://hadleyserver.metoffice.gov.uk/wmolc/) and contributing to CMIP6-DCPP (Decadal Climate Prediction Project).

Using CERSAT sea-ice concentrations to evaluate current decadal climate predictions

A standard procedure in the context of (climate) prediction is the verification of the forecasts, i.e. an assessment of actual forecast skill. This is done by quantitatively comparing the results of forecasts performed in the past with observed values. The huge (computational) effort within DCPP to produce so-called hindcasts back to the 1960s (DCPP component A) enables us to do this.

New high quality observational products are a requirement in this context, especially if they cover periods or regions that are sparsely sampled by other observations. The CERSAT dataset of sea-ice concentrations - part of the iAOS - is such an example, providing daily sea-ice concentrations in a high spatial resolution of 12.5km.
This dataset was used to compute the total Northern Hemisphere (NH) sea-ice area. Fig. 1 shows the interannual timeseries for the mean NH sea-ice area in September when the sea-ice area typically reaches its annual minimum in the Arctic. The CERSAT-timeseries is shown in black and compared with that of another observational dataset, the OSI-450 (gray) product OSI SAF Global Sea-Ice Concentration Climate Data Record, release 2). Both timeseries are very similar, however some differences are visible, too, especially in the years 2009-2011 and 2013. The different colored lines in Fig. 1 represent the September averages for the respective first forecast year (that means 11 months after initialization) of our decadal predictions. Please note that the individual values of the 15 ensemble members are reconstructed to time series for visualization in Fig. 1 even though they are results of distinct forecasts and hence independent of each other. The ensemble mean is plotted in bright green. A typical deterministic skill assessment in such a case is to calculate the (anomaly) correlation coefficient between the forecast ensemble mean and the observations. Making use of CERSAT sea-ice concentrations as observational reference yields a correlation coefficient of 0.83 for a prediction of September NH sea-ice area with this lead-time of 11 months. This may seem as a very positive result.

However, it becomes obvious from Fig. 1 that most of the signal over the period considered (1992-2020) is originating from the downward trend associated with global warming. Analysis of an ensemble of "un-initialized" CMIP6-historical simulations (see Fig. 2) reveals that in that case their ensemble mean features a correlation coefficient of 0.82 when compared with the CERSAT data. The benefit from initializing climate predictions with the actual climate state as done for the SMHI/DMI decadal prediction system hence is rather limited for the specific parameter September NH sea-ice area over a lead time of 11 months.

An introduction of the SMHI/DMI decadal climate prediction system including first assessments of skill has been published (Tian et al. 2021). A more general and global skill assessment with particular focus on Arctic sea-ice is currently in preparation (Karami et al., in prep.).

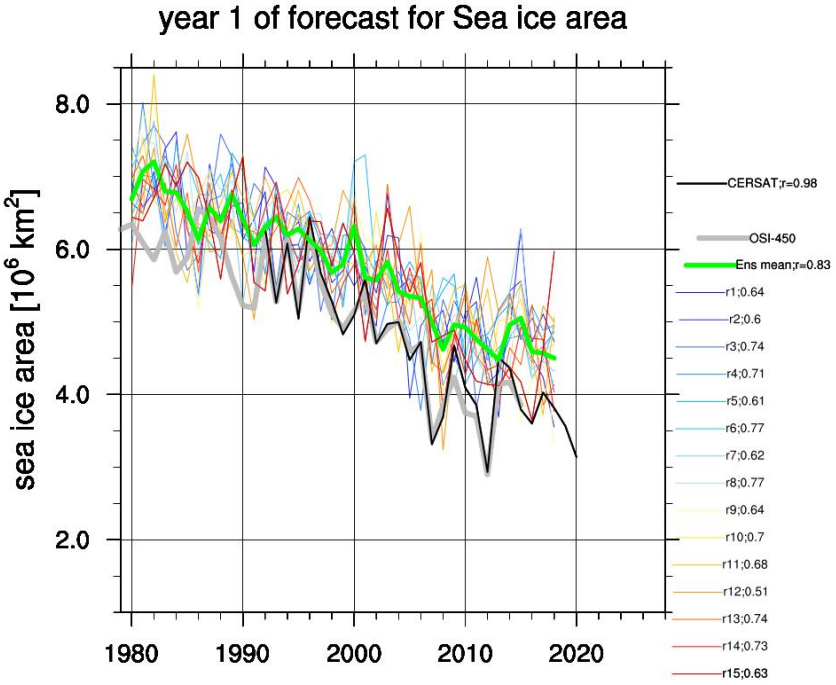

Figure 1. NH sea-ice area in September according to CERSAT dataset (black line) and OSI-450 (grey line) as well as the year 1 predictions (lead time 11 months) according to the 15 ensemble members of the SMHI/DMI decadal prediction system (colored lines) and their ensemble mean (green line)

Ongoing work towards an improved climate prediction system

In parallel to annually producing quasi-operational decadal predictions with the system briefly described above and in D6.1, SMHI works on developing a new improved climate prediction system, which is a continued development since the system for CMIP6-DCPP that is outlined above. The particularity of this system is the performance of coupled assimilation simulations, that means transient coupled AOGCM-simulations that are constantly updated with information about the real world's climate evolution. The setup currently found to yield promising results, assimilates monthly mean sea-surface temperatures (starting in 1900 based on HadISST1) in

the ocean model component and 6-hourly instantaneous fields (linearly interpolated in between) of low-level atmospheric vorticity and divergence which are spectral representations of the horizontal wind components. The assimilation of these atmospheric fields is started in 1950 and based on ECMWF's most recent reanalysis ERA5 (Hersbach *et al.,* 2020) and its backward extension. All fields are assimilated as anomalies to retain the assimilation results close to the preferred model attractor. This is done to mitigate the risks of model drifts after starting the model from initialization fields derived from the assimilation run but switching into the free-running prediction mode.

It should be noted that EC-Earth3 in its current standard configuration does not feature any means of directly assimilating sea-ice information at the time of simulation. The project partner BSC developed and implemented such an option during the course of INTAROS (see Sec. 4 and D6.1). For this reason, SMHI did not make use of CERSAT or any other sea-ice product in the assimilation. Based on the findings of the INTAROS-partners (see Sec. 4 & 5) SMHI may adapt its assimilation strategy in the future.

However, we made use of the CERSAT sea-ice concentrations as an independent reference dataset for evaluating the results of the assimilation runs. Fig. 2 shows again the September mean NH sea-ice area as derived from the CERSAT-product (red line), but now compared to an ensemble of 10 CMIP6-historical simulations (grey) and an ensemble of 5 assimilation runs (blue).

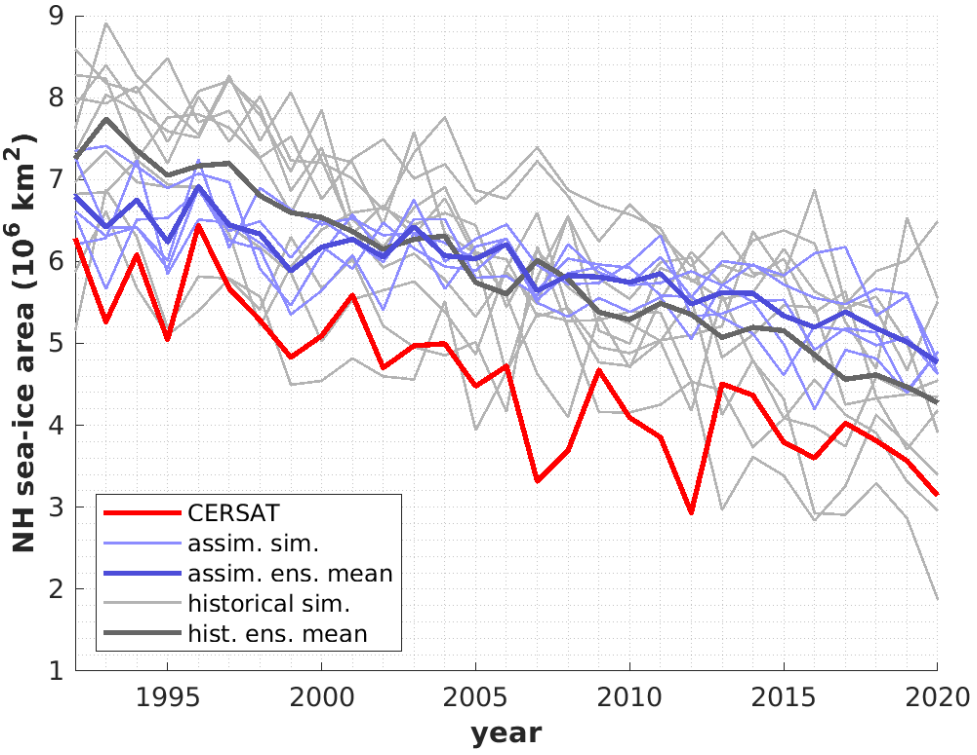

Figure 2. NH September sea-ice area according to CERSAT observational product (red line) as well as an ensemble of free running EC-Earth simulations (grey lines; following CMIP6-historical protocol and SSP2-4.5 after 2014) and a new set of assimilation experiments (blue lines) that assimilate anomalies of SST and low-level winds in the atmosphere

While the assimilation runs feature a somehow smaller trend (-0.05*10⁶ km²/a) over the period 1992-2020 when compared to the CERSAT-observations (-0.09*10⁶ km²/a) and the historical

ensemble (-0.11*10^6 km^2/a), the interannual variability of the assimilation ensemble mean matches the observations quite well, even though with substantially reduced magnitude. The correlation between the assimilation ensemble mean and CERSAT is 0.90 when considering the raw values (including the warming trends), compared with 0.82 for the historical ensemble. Focusing on the interannual variability by linearly detrending the data eliminates any skill of the historical ensemble (correlation of -0.16) while the assimilation ensemble still features a correlation of 0.58. This confirms our expectation that the assimilation of Sea Surface Temperature (SST)-anomalies (in ice-free regions only) and surface-near winds is sufficient to represent the NH sea-ice area reasonably well in our model. The impact on other variables and domains that are not directly subject to data assimilation is currently analyzed. It further needs to be shown if this approach is sufficient to generate better initial conditions used for potentially improved decadal climate predictions.

4. Seasonal predictions making use of assimilating CERSAT sea-ice concentrations (BSC-contribution)

The smaller subset of seasonal hindcasts from BSC presented in D6.1 (Sec. 4) has been extended with additional members (30 in total) to also include the assimilation of SIC from OSISAFv2 (*Lavergne et al., 2019*, 10 members) and ORAS5 (*Zuo et al., 2019*, 10 members), in addition to the original SICs from CERSAT (*Girard-Ardhuin et al., 2018*, 10 members). This was done to both isolate the predictable signal common to all products (i.e., partly circumventing observational uncertainties) and to test the sensitivity of the forecast skill to the assimilated product (see Table 2 for more details). Additionally, a thorough assessment of skill in the Arctic and mid-latitude has been carried out, and now complements the initial analysis in D6.1, which was focused only on mean biases. In terms of seasonal forecast skill, SIC assimilation offers no improvement with respect to no SIC assimilation in the (November 1st initialized) winter/spring hindcasts, but has important benefits in the (May 1st initialized) summer/fall hindcasts. For this reason, only summer/fall hindcasts are discussed in the following.

Table 2: EC-Earth3.3 forecast system (BSC) description

Hindcasts - 7 months	***Model***	***Atmosphere initial conditions***	***Ocean and sea-ice initial conditions***	***Restoring timescales***
NOSIC-ASSIM May 1st and Nov 1st initializations 1992-2019 30 members	EC-Earth3.3 NEMO3.6 - LIM3 - IFS c36r4 - H-Tessel	ERA5 (interpolated)	NEMO3.6-LIM3 reconstruction forced by ERA5 surface fluxes, restoring T and S.	Surface T and S: ~ 10 days. Subsurface T and S: ~ 3 days below mixed layer decreasing with depth.
SIC-ASSIM May 1st and Nov 1st initializations 1992-2019 30 members	EC-Earth3.3 NEMO3.6 - LIM3 - IFS c36r4 - H-Tessel	ERA5 (interpolated)	NEMO3.6-LIM3 reconstruction forced by ERA5 surface fluxes, restoring T, S and **SIC (CERSAT, ORAS5 and OSISAFv2, 10 members each)**	Surface T and S: ~ 10 days. Subsurface T and S: ~ 3 days below mixed-layer decreasing with depth. **SIC: ~3 days**

Summer/fall hindcasts

Regardless of the observational sea-ice product assimilated, the hindcasts with SIC assimilation (SIC-ASSIM) initialized every 1st of May in the period 1992-2019 show a consistent and significant improvement with respect to NOSIC-ASSIM, in forecasting the Arctic sea-ice edge in May, June, July and October (Fig 3a-c), showing the largest differences in May, but barely any difference in most of the late summer months (JAS). The small, but significant improvement in the fall is likely due to a well-known spring-fall reemergence mechanism of Arctic sea-ice (*Bushuk et al., 2017*). Interestingly, May, June, and JAS sea surface temperature (SST) show larger skill (in terms of anomaly correlation coefficients) in SIC-ASSIM than NOSIC-ASSIM in the central North Atlantic, far from the sea-ice edge (Fig 3d-f, purple box). Assimilation of each SIC product gives similar results in the North Atlantic region (not shown). This feature is robust regardless of the SIC product assimilated, which suggests that improved sea-ice initialization through assimilation is behind the improvements, the small ones seen in May and the enhanced improvements in the subsequent months (maximum correlation differences occur in June-September).

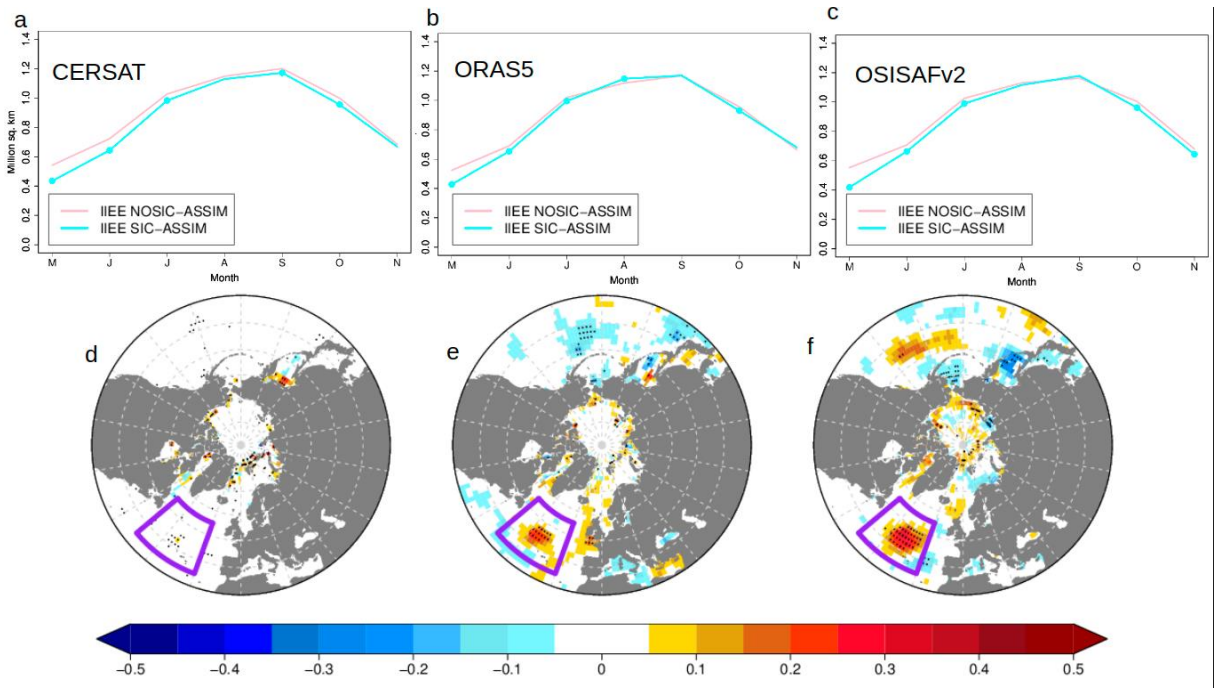

Figure 3: Mean 1992-2019 integrated Arctic sea-ice edge error (IIEE) as a function of forecast month in NOSIC-ASSIM (light red) and SIC-ASSIM (light blue) hindcasts for members (a) 1-10, (b) 11-20 and (c) 21-30. SIC-ASSIM members 1-10, 11-20, and 21-30 are initialized with assimilation of CERSAT, ORAS5 and OSISAFv2 SICs, respectively. Difference in SST skill (anomaly correlation) between SIC-ASSIM and NOSIC-ASSIM in (d) May, (e) June and (f) JAS in the 30-member ensemble. The observational reference is NSIDC for SIC and HadISSTv1.1 for SST. Dots on lines (a-c) and on the maps (d-f) indicate statistically significant differences (95% confidence) between SIC-ASSIM and NOSIC-ASSIM.

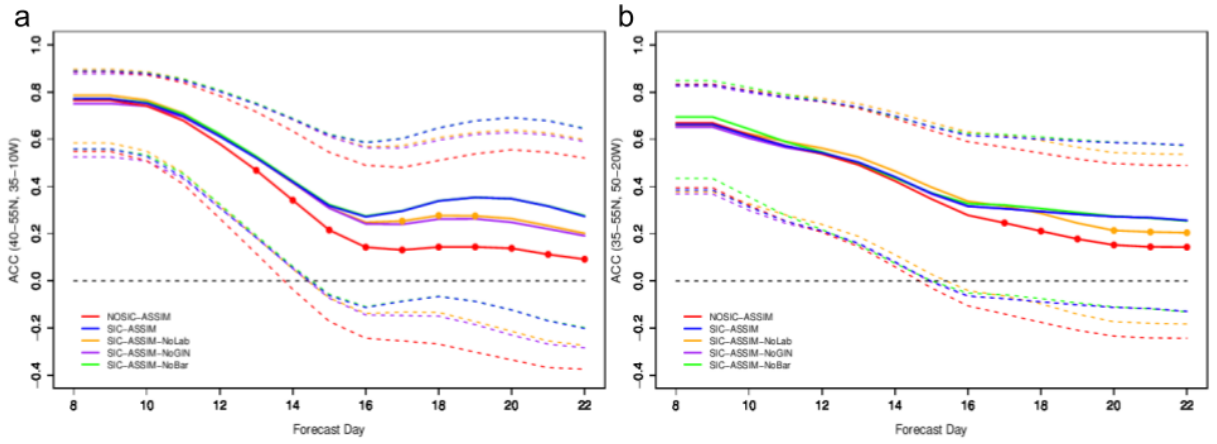

Figure 4: (a) GPH500 skill (anomaly correlation) in the North Atlantic of running bi-weekly mean in May of NOSIC-ASSIM (red), SIC-ASSIM (blue), and SIC-ASSIM without the sea-ice influence in Labrador-Baffin (yellow), GIN (purple) and Barents (green) hindcasts (See text). (b) The same for TAS. The observational reference is the mean of ERA5, JRA55 and NCEP reanalyzes. Dots on lines indicate statistically significant differences (95% confidence) between SIC-ASSIM and each one of the other lines. Dashed lines indicate the 95% confidence interval.

To gain further insight into how the improved SICs lead to better skill in North Atlantic SSTs, a sub-monthly analysis of skill for geopotential height at 500mb (GPH500) and near surface air temperature (TAS) has been performed. It reveals improved skill in SIC-ASSIM with respect to NOSIC-ASSIM in the North Atlantic region already by forecast weeks 2 and 3 for GPH500 (40-55N,35-10W) and TAS (35-55N,50-20W), respectively (Fig. 4 a, b). Note that the

difference in skill between SIC-ASSIM (blue line) and NOSIC-ASSIM (red line) hindcasts is exclusively caused by SIC assimilation, which allow us to conclude that better initialization of Arctic SICs positively influences North Atlantic SSTs through an atmospheric bridge that develops during the first two weeks of the forecast. To establish if a causal link exists between the improved SIC skill and that in North Atlantic GPH500 and TAS, we follow the method described in *Acosta Navarro et al. (2020)*, which consists of linearly regressing out the variability of the leading variable before the skill for the driven variable is evaluated. By comparing the skill in the original SIC-ASSIM hindcasts with that of the synthetic hindcasts in which SIC variability is regressed out, we can thus determine whether and how much the leading variable contributes to the skill of the driven one. We have applied this approach for the sea-ice area at time of initialization (on May 1st) in three separate regions: the Labrador-Baffin (yellow line), Greenland-Iceland-Norwegian (GIN) (purple line) and Barents (green line) Seas (Fig. 4 a, b). Removing the sea-ice signal from SIC-ASSIM reveals that both, GIN and Labrador-Baffin Seas reduce the GPH500 sub-monthly skill in the North Atlantic, which makes these synthetic forecasts closer to NOSIC-ASSIM. In the case of TAS, only Labrador-Baffin Seas appear to have a significant impact on the forecasts. The skill degradation caused on one hand by the lack of SIC assimilation, and on the other by the statistical removal of sea-ice signal from given regions, leads us to conclude that the state of sea-ice in the GIN, but especially Labrador-Baffin Seas affect the atmosphere in spring and matters when it comes to SST predictability throughout the summer and early fall.

The higher skill of SIC-ASSIM than NOSIC-ASSIM for SSTs in the North Atlantic region, initially driven by better atmospheric circulation in May (Fig 4), persists well until September (Fig 5 a). This persistent improvement also leads to better GPH500 forecasts in JAS in the North Atlantic and Eurasian regions, a result that is confirmed by two independent analyses. Firstly, by comparing the JAS skill in SIC-ASSIM hindcasts with a synthetic hindcast without the signal explained by the North Atlantic SST index in JAS (Fig 5 b). The skill in the synthetic hindcasts is computed using the residual of SIC-ASSIM after linearly regressing out the North Atlantic SST index (JAS), and this is done for each member separately (for more details see Acosta Navarro et al., 2020). This difference between original and synthetic SIC-ASSIM hindcasts indicates the regions where the JAS SST index improves (red/yellow) or degrades (blue) the skill. Secondly, the skill gain from the SIC assimilation (computed as the difference in anomaly correlations of SIC-ASSIM and NOSIC-ASSIM) shows a remarkable similarity (Fig. 5 b, c) in the North Atlantic and Eurasia, giving not only confidence in the results, but also supporting the importance of Arctic SIC assimilation for summer/fall forecasts.

The mechanism connecting springtime SICs with JAS atmospheric circulation is a two-step mechanism: 1) a fast (sub-monthly timescales) atmospheric bridge develops in May, and connects the sea-ice in the North Atlantic sector of the Arctic with the SSTs in the central North Atlantic; and 2) the improved SSTs in the central North Atlantic persist from May until September, and via turbulent heat fluxes (not shown), improve the local and remote (Eurasia) atmospheric circulation during JAS, ASO and SON, improving as well the prediction skill of surface air temperature and precipitation (not shown).

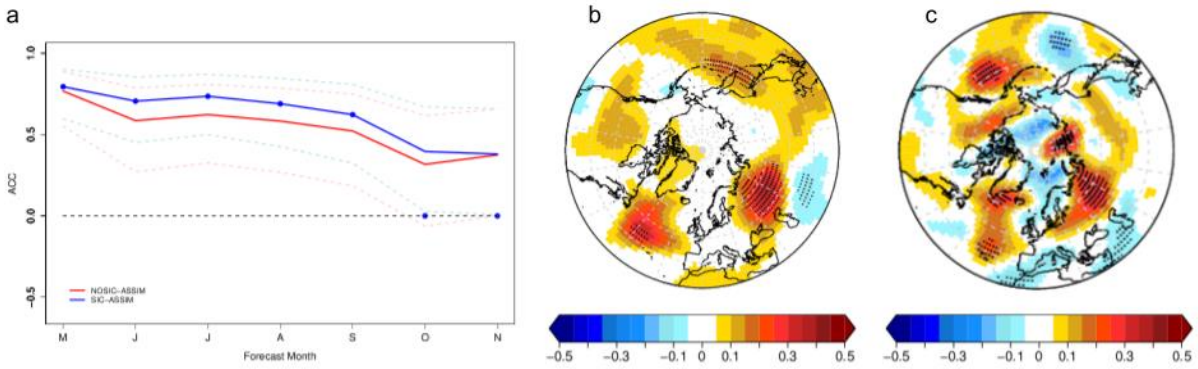

Figure 5: (a) Monthly SST skill (anomaly correlation) in the North Atlantic in NOSIC-ASSIM (red) and SIC-ASSIM (blue). (b) Difference in GPH500 skill (anomaly correlation) in JAS between SIC-ASSIM and SIC-ASSIM without the influence of North Atlantic SSTs in JAS (see text). (c) Difference in GPH500 skill (anomaly correlation) in JAS between SIC-ASSIM and NOSIC-ASSIM. The observational reference is HadISSTv1.1 for SST and the mean of ERA5, JRA55 and NCEP reanalyzes for GPH500. Dots on the line (a) and on the map (c) indicate statistically significant differences (95% confidence) between SIC-ASSIM and NOSIC-ASSIM. Dots in (b) indicate the same, but for the differences between SIC-ASSIM and SIC-ASSIM without the North Atlantic SST signal (JAS).

5. Seasonal/decadal climate predictions making use of assimilating C2SMOS sea-ice thickness (NERSC contribution)

In D6.1, we have used the Norwegian Climate prediction Model (NorCPM; developed at NERSC) and show that assimilation of ocean data could already achieve skillful prediction in some regions of the Arctic (e.g., in the Barents Sea, *Wang et al.* 2019, *Dai et al.* 2020, *Bethke et al.* 2021) during winter months, as ocean heat content can prevent the formation of sea ice. The assimilation method "advance ensemble Kalman Filter (EnKF)" has been utilized in NorCPM. With assimilation of SIC in addition, skill near the Arctic Shelves emerges and skill extend towards the summertime (*Kimmritz et al.* 2019, K19 in the following) as the approach can skillfully initialize regional thickness anomalies. Hence, assimilation of ocean data (e.g., *Bethke et al.* 2021, see Fig. 6) and/or with SIC in addition (K19) can reduce drastically the bias of SIT when strongly coupled data assimilation is enabled (The system allows ocean data to correct the sea ice state and/ vice versa if SIC is assimilated).

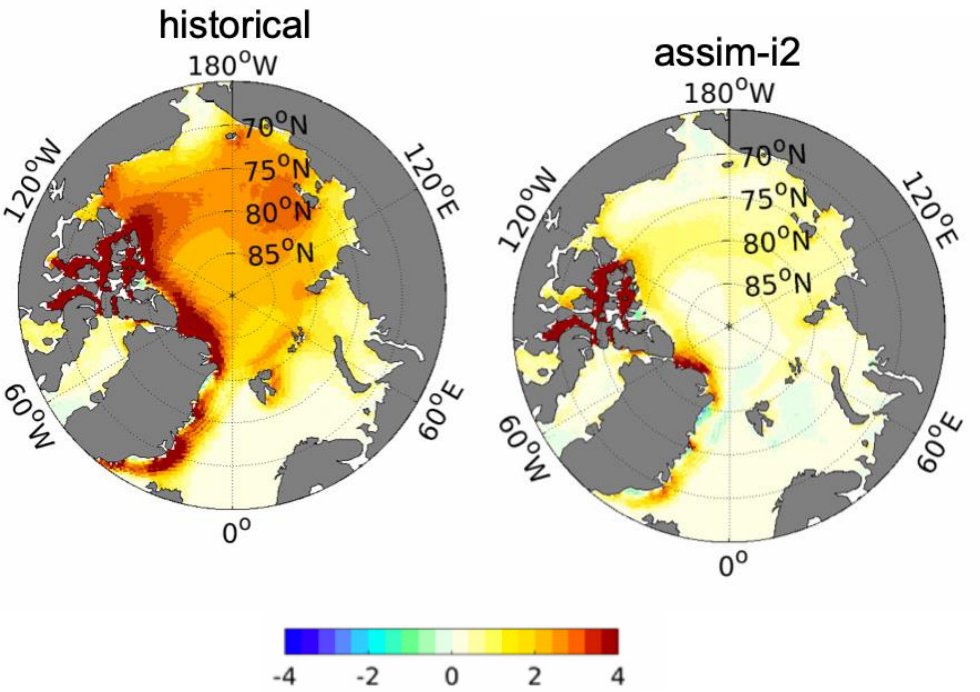

Figure 6. November-March climatological bias of sea-ice thickness (in m) in a free historical ensemble, and in an assimilation experiment with ocean observation only. The observational reference combines C2SMOS (Ricker et al. 2017), Cryostat2 and Envisat (Hendricks et al. 2018) over the period 2002--2018.

However, the implementation in K19 yields a slight degradation for ocean heat content (OHC) at mid latitude. For D6.11 we aim to 1) rectify this limitation and 2) complement this system with assimilation of ice thickness. NorCPM uses anomaly assimilation meaning that the climatological bias of the observed quantity is left unchanged- an approach that limits assimilation shocks. As such, we needed to construct the climatological reference of ice thickness with the revised system.

The degradation in mid-latitude OHC was identified to be caused by an assimilation set up. For assimilation of ice concentration and sea surface temperature, the impact of assimilation was limited to the mixed layer in this particular set-up, while the impact of a full depth assimilation has been demonstrated in other versions of the system (*Counillon et al.* 2014, *Counillon et al.* 2016). We have repeated the experiment of K19 but this time for the period 2002-2020 and with update of the full ocean state, to be able to construct the climatology of SIT.

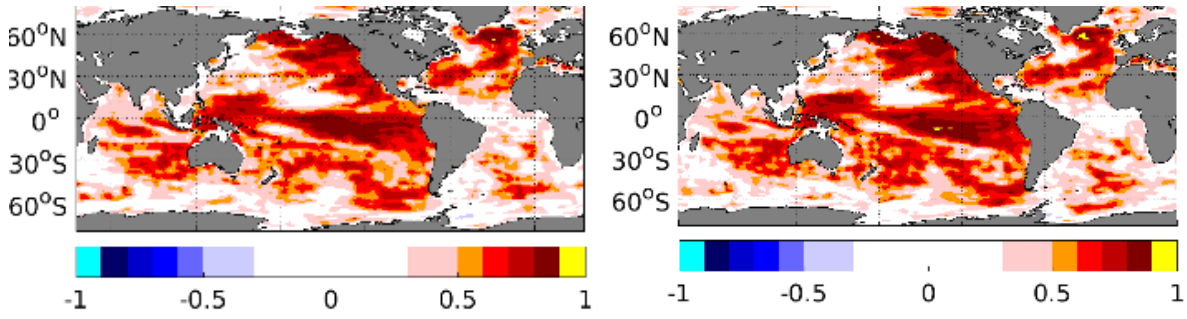

Figure 7. Correlation skill of 200-meter Ocean Heat Content computed against EN4 objective analysis for the period 2002-2019 in the version of NorCPM with ocean observation only (left) and ocean & sea-ice concentration (right).

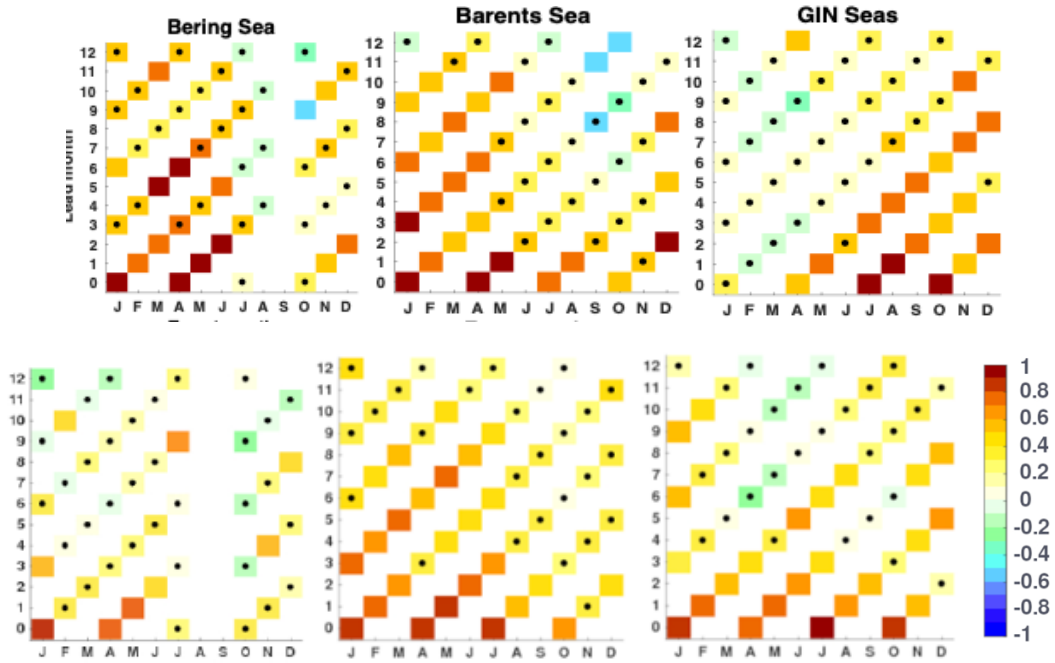

Figure 8. Detrended correlations of the initialized retrospective predictions with the sea-ice extent derived from the NOAA OISSTV2 retrievals. The y-axis is the lead months, and the x-axis is the target months. The upper row panels shows results from the new system while the lower panels is as in K19 using HadiSST2 in 3 different regions. Dots denotes insignificant correlations using a significance level of 5%.

The degradation of skill in OHC is no longer visible and the system with assimilation of ocean and sea-ice concentration performs better than the system with ocean data everywhere (see Fig. 7). It is hard to directly compare the performance of sea-ice extent with that of K19 because the period of study is different (1980-2010 in K19 and 2002-2019 now), but the performance of the new system is very comparable (see Fig. 8). Still there is improved skill in some regions (Barents Sea, Kara Sea (not shown), Bering Seas) and in some other regions the skill seems to be now more prominent in summer than in winter (Greenland-Iceland-Norway aka GIN).

We are currently investigating whether these changes are due to the improvement in the version of the system or due to a modulation of the prediction skill with climate change (e.g., *Årthun et al.* 2021).

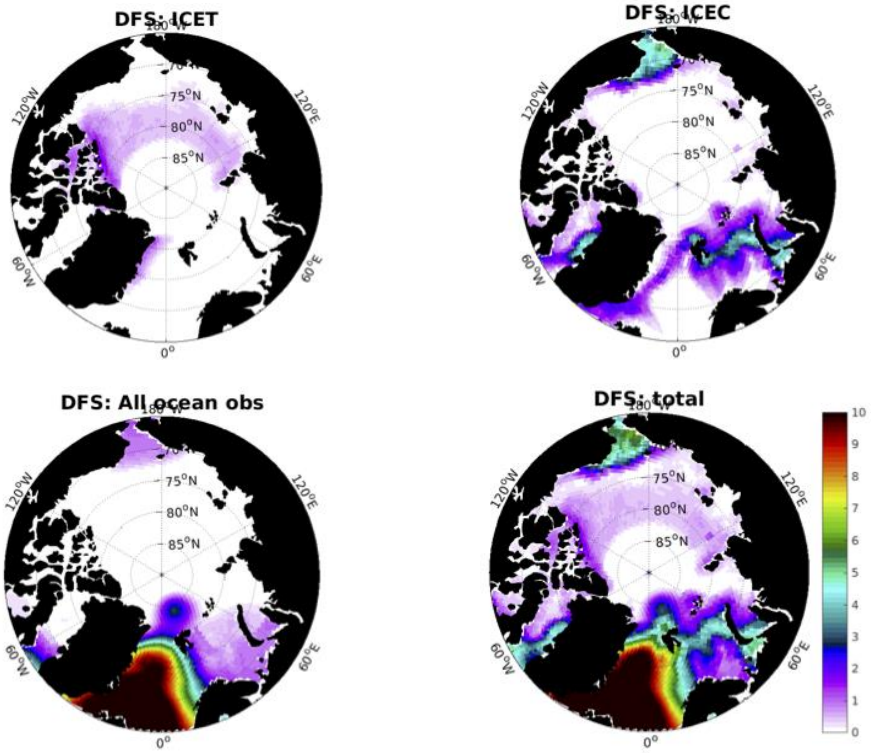

Figure 9. Degree of Freedom of Signal of the ice thickness (from ENVISAT CCI 2.2), ice concentration, all ocean observations and the total by assimilation in November 2002.

For assimilation of sea-ice thickness data we have used the ENVISAT CCI 2.2 (*Hendricks et al.* 2018) from November 2002 to March 2010 and the C2SMOS (*Ricker et al.* 2017) version V203 from November 2010 to 2020. The data is only available for the wintertime, and we have discarded the transition months October and April. The accuracy of this data is lower during the transition month, and we have rejected it to be cautious - it has caused artefacts other systems (*Xie et al.* 2018). Envisat and CS2SMOS SIT are not fully consistent with CS2SMOS providing more thin ice, especially in the marginal sea-ice zones. Assimilation of the anomalies of both products ensures a smooth transition. The climatology period for computing anomaly assimilation for ENVISAT is 2002-2012 and 2010-2019 for C2SMOS. For ENVISAT CCI 2.2 we have used the provider observation error uncertainty in the monthly average. For C2SMOS the data is provided in daily average, and we have computed monthly average from the daily average and observation error as their harmonic mean.

To quantify the relative influence of ice thickness data we use the degree of freedom of the signal (*Sakov et al.* 2012) that quantifies the number of degrees of freedom that is reduced by assimilation of each observation type. This number is limited by ensemble size (i.e., less than 30), but one expects with the current system not to exceed 10. We show the cumulative impact of all ocean observations together (SST, temperature and salinity profiles), ice concentration (ICEC) and ice thickness (ICET). We notice that the influence of observations is much larger outside of the Arctic than inside and that exemplifies the need for more and novel observations there. In the Arctic, ice concentration has a large influence near the ice edge but none inside the Arctic. Ice thickness provides a very complementary -albeit comparatively smaller in amplitude. This data set allows a constraint on internal variability also inside the central Arctic. Fig. 9 shows the result for ENVISAT sea-ice thickness product and Fig. 10 shows the same for

C2SMOS data set. We can see how the influence of C2SMOS is larger than ENVISAT, as CRYOSAT is better tailored for retrieving thick SIT and because it is combined with SMOS that can retrieve thin ice thickness. As a matter of fact, SIT in 2011 become a more important data set for constraining internal variability error than SIC. Another striking difference is the increase of importance of temperature and salinity profile in the Arctic with the emergence of ice-tethered profilers.

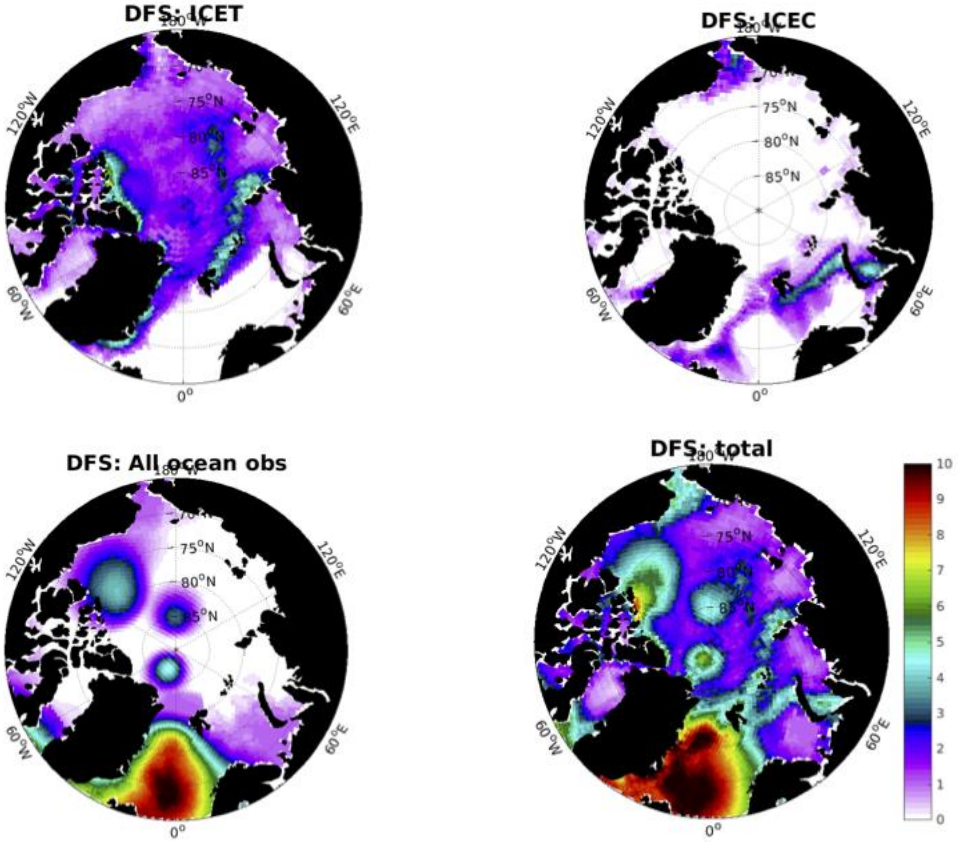

Figure 10. Degree of Freedom of Signal of the ice thickness (from C2SMOS), ice concentration, all ocean observations, and the total by assimilation in November 2011.

In Fig. 11, we show the time series of the assimilation diagnostic. We can notice that the Root Mean Square Error (RMSE) of ice thickness reduces from over 1.5 m to below 1 m during the ENVISAT era and fluctuated between 0.5 m and 0.75 during the C2SMOS era. We can notice how error grows up slowly as sea-ice thickness observations are missing during summertime. A very important aspect of an ensemble prediction system is its reliability - i.e., its capacity to predict its error. Therefore, we are adding the estimated error (with a magenta line), which in a well-balanced system should be of comparable level to the RMSE. We can see that this is nicely satisfied during the Envisat-era but that the estimated error is too low compared to the RMSE during the C2SMOS era. In the latest attempt, we had inflated the observation error from the data provider by a factor 2 but the reliability is still too low and further iteration will need to be carried out in the future. sea-ice

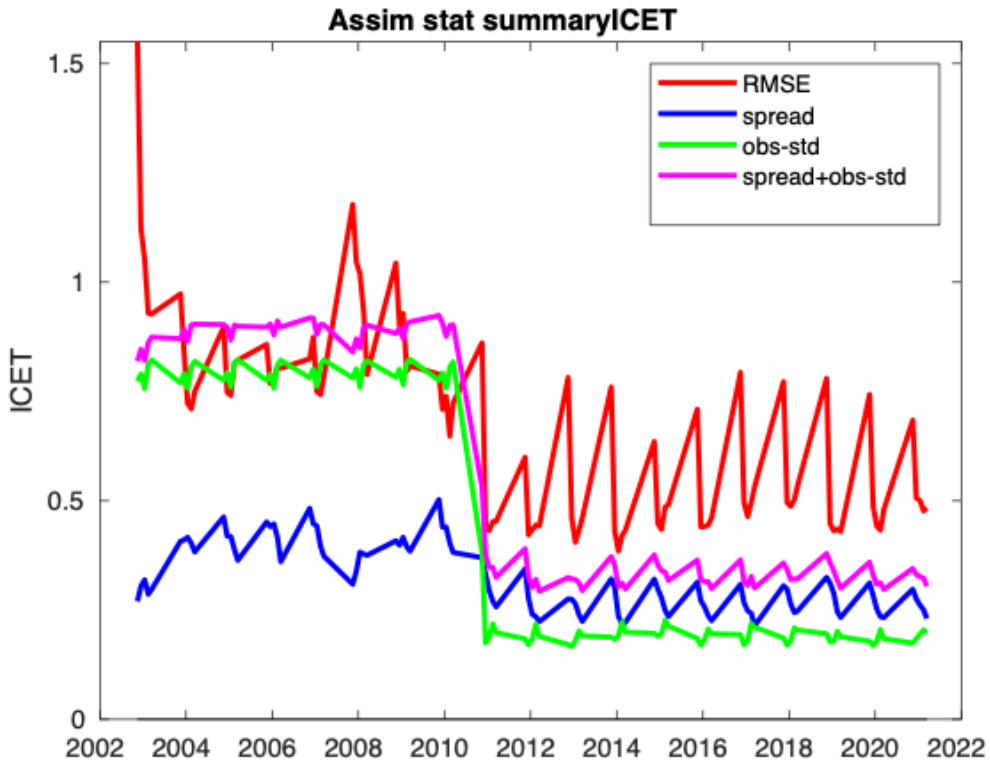

Figure 11. Sea ice thickness as result of assimilation diagnostic of the reanalysis with assimilation of SIT. The red line is the RMSE vs assimilated data before analysis, the green line is the observation standard deviation (in meter). The blue line is the ensemble spread (model uncertainty). The magenta line is the estimated total error (which is √(〖spread 〗 ^2+ 〖obs_std〗 ^2).

6. Impact of hydrological observations for the prediction of spring floods, river ice breakup and freshwater flow to the Artic Ocean (SMHI contribution)

Objectives

The aim of this activity is to demonstrate the added value of the integrated arctic observation systems (iAOS) for enhancing and make available hydrological model predictions for the major Arctic rivers. The main objective is to combine the river discharge data from the Arctic Hydrological Cycle Observing system (Arctic-HYCOS) - that was assessed and enhanced in INTAROS WP2 – with the pan-Arctic hydrological model Arctic-HYPE provided by SMHI (http://hypeweb.smhi.se), to predict and monitor fresh water inflow to the Arctic Ocean and changes in Arctic hydrological regimes. The demonstration case consists of an operational application of the Arctic-HYPE model providing daily analyses of the last 60 days, and medium range forecast of the coming 10 days. The Arctic-HYPE analyses and forecasts are stored at SMHI open data repositories and will be made available using OPeNDAP server technology. Arctic-HYCOS observations are accessed by the operational service using the tools and metadata provided by INTAROS WP2 catalogue (https://catalog-intaros.nersc.no/dataset/arctic-hycos-hydrological-data/).

One of the goals is to demonstrate the improvement of the pan-Arctic hydrological analyses and forecasts by assimilating the river discharge data in the operational Arctic-HYPE application. A second goal is to demonstrate the ability to build user-tailored data products based on the Arctic-HYPE data accessed through an OPeNDAP server. The latter will be illustrated by a use-case in Republic of Sacha (Yakutia), in Far-East Russia, where a sub-set of the Arctic-HYPE model is used for spring flood and river ice breakup forecasting in the major Yakutia rivers.

Pan-Arctic hydrological model Arctic-HYPE

Arctic-HYPE version 4.2 is a new pan-Arctic application of the hydrological model HYPE (Hydrological Predictions for the Environment; *Lindström et al*. 2010; SMHI http://hypeweb.smhi.se) simulating water balance of glaciers, snow, soil, lakes and rivers, representing processes such as runoff, river discharge and water level, and river ice growth, melt and breakup. It is based on Arctic-HYPE version 3.1 which was previously applied to the Lena River basin (*Gelfan et al.,* 2017) and the Hudson Bay complex (MacDonald et al, 2018). The model domain covers the land areas draining into the Arctic Ocean and related water bodies in the northern seas as defined in Fig. 12. The total model area is 26 Mkm^2 distributed on 34421 sub-basins with a median area of 623 km^2. Main improvements compared to Arctic-HYPE v3.1 are a) improved sub-basin delineation based on the World-wide HYPE (*Arheimer et al*, 2020) with further adjustments to the Arctic-HYCOS station locations, b) a new parameterization of frozen soil impact on runoff generation, c) overall improved calibration of water balance and cryosphere processes including evaporation, snow, and river ice using primarily local observations from Yakutia river gauges and research basins. Daily forecast for the next 10 days is produced with meteorological forcing data from the ECMWF deterministic medium range weather forecasts. The forecast model is initialized by an analysis of the previous 60 days, forced by the HydroGFD v3 temperature and precipitation data (Berg et al, 2017), in which the

Arctic-HYCOS data will be assimilated to improve the initialization. The historical simulations include daily river discharge for the period 1979 to 2019.

Arctic-HYPE v4.2 OPeNDAP data service

The previous version of the Arctic-HYPE model (v3.1) was disseminated through an interactive map browser service at http://hypeweb.smhi.se. Users could download data from one sub-basin at the time by selecting the location in the web map interface. All data were openly available; however, the limitation of data access through the interactive map browser prevented structured data access, access of larger parts of the model domain. Data from the full model domain was available for licensed users, but only through a FTP server, with the backside that users had to download data from the full data domain before extracteing their sub-domain of interest.

To improve the Arctic-HYPE data access, and to open up for structured retrieval through the iAOS, a new data dissemination service has been developed using a THREDDS data server implementing the OPeNDAP protocol. The server will be hosted at www.smhi.se providing Arctic-HYPE data in NETCDF format following the CF-convention (http://cfconventions.org/). The operational implementation of the server is still on hold due to security measures following the COVID-19 pandemic, but it is expected to be online later during 2021.

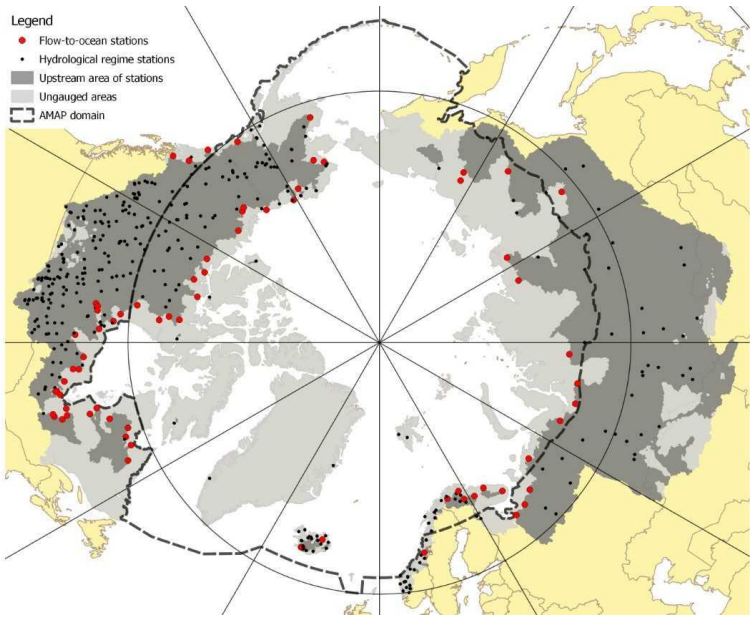

Figure 12. Pan-Arctic drainage basin of the Arctic Ocean and related water bodies in the northern seas (PADB) as represented in the Arctic-HYPE model (grey shaded areas) and the locations of the Arctic-HYCOS river discharge stations (red and black dots); the dark-grey area represent the drainage basin of the observational network, whereas the light-grey area represent the ungauged part of the PADB. Drainage basin of the Arctic Ocean and related water bodies in the northern seas as represented in the Arctic-HYPE model (light grey), the location of the Arctic-HYCOS stations and their upstream drainage basins (dark grey).

Yakutia spring flood and river ice breakup forecasting

A sub-set of the Arctic-HYPE model covering the Republic of Sacha (Yakutia) in Far East Russia, was used to develop a spring flood and river ice breakup forecasting service (Fig. 13). This use-case is developed in collaboration with the HYPE-ERAS and Hydrology TEP projects

with partners from Russian and Japan, funded through a Belmont Forum Arctic II collaborative research action and the European Space Agency, respectively. For the spring flood 2020, the new version of Arctic-HYPE (v4.2) was implemented to run operationally in the SMHI production system, publishing the outputs of the 10-day forecast and 60-day analysis daily in an internal offline version of the OPenDAP server. Results were extracted for selected locations in the Yakutia domain as exemplified in Figure 3, which show the forecast issued 2020-05-08 for the Lena River at Kangalassy, just upstream of the city of Yakutsk. Similar forecast plots were produced for about 90 points of interest (Fig. 13). The forecast points were selected based on availability of in-situ observation as well as stakeholder interest. A summary of the forecasts providing information on the expected river ice breakup dates, and river water level tendencies were made every day by collaborators at the Melnikov Permafrost Institute in Yakutsk and communicated with the local stakeholders. The 2020 river ice breakup in the Lena River at Yakutsk took place on the 11th of May, which correctly predicted by the Arctic-HYPE forecast issued on the 8th of May (Fig. 14). A few days after the on-set of ice flow in the river, an ice jam was developed in the Lena River at Kangalassy; downstream of Yakutsk; with flooding of parts of the city.

This use-case illustrates how the Arctic-HYPE data may be used in a future application when it is made available in the open OPeNDAP server. It should also be noted that in this example, observations of water level and river ice conditions from Roshydromet were collected in collaboration with local stakeholders and used for verification of the hindcast model results. River ice, water level and river discharge data set from historical period 2008-2017 were used to establish first of all stage-discharge relationships to transform the discharge simulated by the model to water level predictions, and secondly long-term statistics on most efficient river ice porosity trigger break up and ice flow conditions (Fig. 14). These data are not part of the iAOS, but the use-case illustrates the situation where a local user can combine the open available data provided by the iAOS with their own data to produce enhanced forecasting products.

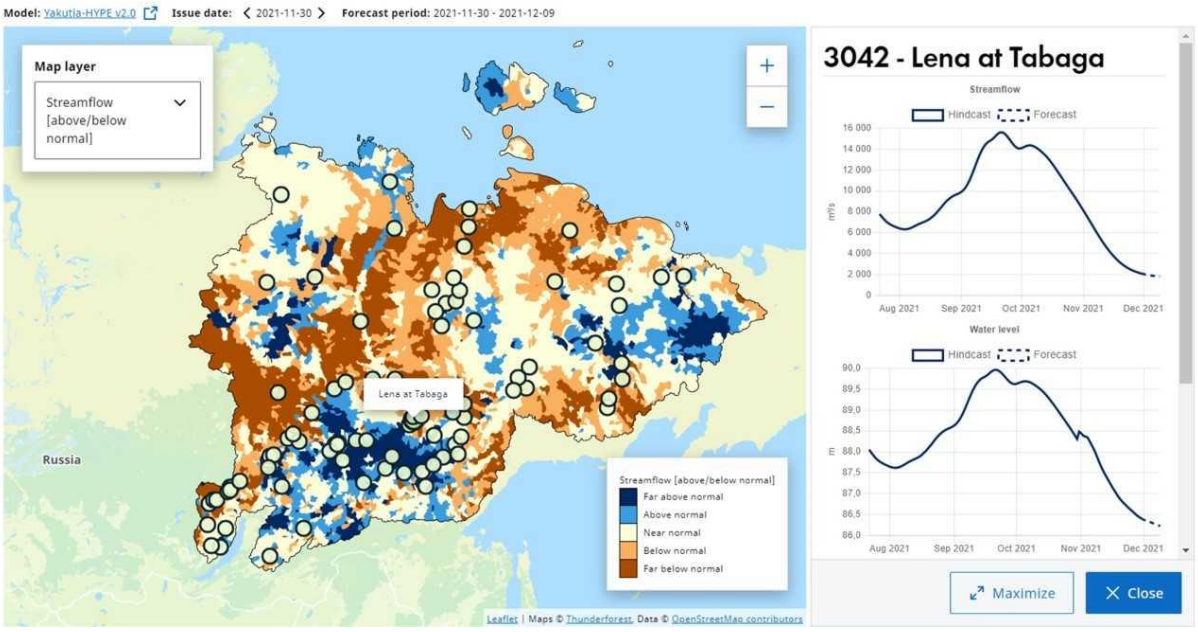

Figure 13. Impression of the HYPE-ERAS forecast service available at http://hype-eras.org/forecasts showing a map of the Yakutia-HYPE model, location of forecast points (white markers), and time series of river discharge and water level for a selected forecast point.

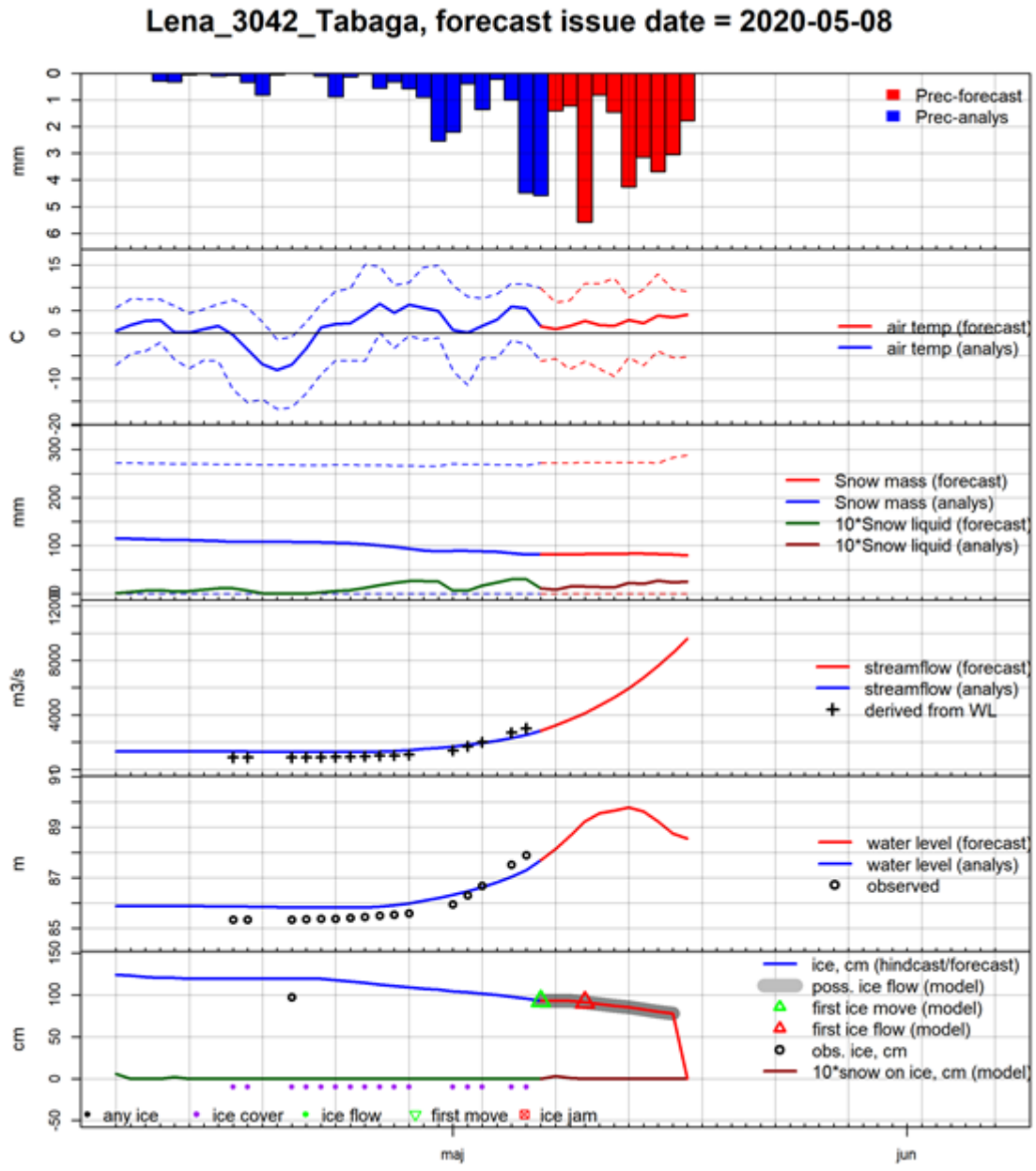

Figure 14. Arctic-HYPE forecast for Lena River at Tabaga (upstream of the city of Yakutsk), forecast issue date 2020-05-08. Hindcast and available observations (blue lines and symbols) and forecast (red lines and symbols), from the top, 1) precipitation in the upstream area (mm), 2) mean air temperature (dotted lines indicate minimum and maximum), 3): snow water equivalent (mm), 4): river discharge (m3/s), 5t) river water level (m), 6) ice thickness (cm) and so-called ice-processes.

7. Summary

This report summarizes results of the work performed in Task 6.1 and gives recommendations on how to use different observational or reanalysis data sets, and what effects to be expected. The main goal of the task was to improve the skill of climate predictions, by means of investigating the benefits related to the exploitation of Arctic data collected in iAOS. Benefits for the climate modelling community translate directly into user benefits also for stakeholders of climate services such as the European Copernicus Climate Change Service (C3S).

Climate prediction has gone through various improvements during the last 10 years, with the common goal of increased prediction skill on the seasonal to decadal time scale. Sources of improved skill are seen in initialization methods, improved climate models, size of the prediction ensemble, and a wider usage of observational data in the initialization schemes. Thereby especially observations in the Arctic are expected to boost the development due to an existing under-coverage of that area and due to the sensitive sea-ice cover in the area. Inclusion of Arctic data in initial conditions to start the model from, for climate prediction is expected to improve the prediction skill. In addition, access to Arctic observational data (not used in the initial conditions) allows for model evaluation and skill assessment independent of the initial fields.

Consequently, a key ingredient to skillful seasonal-to-decadal climate prediction is the use of high-quality observational data, that covers a sufficiently long period, typically at least a few decades to robustly test their impact. This emphasizes the need - from a user perspective - to sustain and continue the production of the various iAOS products.

Here we made use of three different datasets provided through the iAOS, developed in the INTAROS project, namely CERSAT sea-ice concentrations, C2SMOS sea-thickness, and Arctic-HYCOS river discharges.

CERSAT sea-ice concentrations were used in two ways: for assessment of prediction skill and for assimilation into initial conditions.

The skill was assessed for the EC-Earth3 quasi-operational decadal climate predictions regarding September Northern Hemisphere sea-ice area for a lead time of 11 months (based on the period 1992-2020; correlation of 0.83), without sea ice concentration in the start fields, and regarding the quality of updated assimilation experiments providing potentially better initial conditions for climate predictions (correlation of 0.9 including long-term trend; 0.58 for detrended data, i.e. interannual variability).

In a separate prediction setup, CERSAT sea-ice concentrations also were assimilated for the EC-Earth3 seasonal climate prediction system. It is shown that the assimilation of sea-ice concentrations does not yield significant benefit for winter seasonal predictions (started on 1 November). However, the assimilation has a remarkable positive impact on summer seasonal predictions (started on 1 May) regarding the sea-ice edge but also regarding remote North Atlantic SSTs. The latter is shown to be the result of a so-called atmospheric bridge translating the improved sea-ice representation via more realistic large-scale atmospheric variability into the SST-signal.

Next, the assimilation method “advance ensemble Kalman Filter (EnKF)“ has been utilized to enhance initial conditions for the Norwegian Climate Prediction Model (NorCPM). The flow dependent property of the method has been shown to be key for carrying joint update of the ocean and sea-ice. The EnKF can handle the non-stationarity of the coupled covariance and allows individual update of the multi-category sea-ice state; the latter being crucial for efficient reduction of error in sea-ice thickness. Based on this knowledge, NorCPM can achieve skillful prediction of sea-ice extent in several regions of the Arctic (improved performance of decadal

prediction at high latitude). Assimilation of ice concentration is shown to further improve performance over the Arctic shelf and the export of sea-ice through the Fram Strait.

Results demonstrates that the complexity of the respective data assimilation method is of importance to optimally use observations that are relatively sparse in the Arctic. NorCPM is currently being tested at higher resolution, and we can benefit from using the high resolution CERSAT sea-ice concentration data set available in INTAROS Data catalogue.

The NorCPM experiments are especially interesting due to the assimilation of SIT. A reanalysis extending from 2002—2021 has been produced combining the ENVISAT-CCI sea-ice thickness data until 2010 and the C2SMOS data set that combines the CRYOSAT data set and the SMOS sea-ice thickness data that is available in INTAROS Data catalog. Sea-ice thickness is shown to be complementary data to ice concentration and hydrographic data (temperature and salinity). Assimilation of ice thickness allows for a substantial reduction of error in sea-ice thickness (compared to the system only assimilating ice concentration). The system reaches an error of about 0.5 meter for the Arctic in winter when observations are available and 0.75 meter when observation are not available during summer. We also show that a careful adjustment of the observation error is needed to avoid degrading the reliability of an ensemble system.

River discharge data from the Arctic-HYCOS observation network were assessed in INTAROS WP2 and is available through the INTAROS data catalogue. It has been used to improve pan-Arctic hydrological analyses and subsequent forecasts with the Arctic-HYPE model. It should be noted that in a first step, the river discharge station locations were used already in the model development phase by controlling the river basin delineation, and that the river discharge time-series were used in sub-sequent model calibration and data assimilation steps. The functionality of this workflow is demonstrated via a use-case in the Republic of Sacha (Yakutia), in Far-East Russia, where a sub-set of the Arctic-HYPE model is used for spring flood and river ice breakup forecasting in the major Yakutia rivers.

8. Future perspectives and lessons learned

Recommendations

Recommendations and lessons learned resulting from Task 6.1 are:

- Assimilation of sea-ice concentrations provide better initial conditions for climate predictions that lead to improved prediction skill for time scales from seasons a year. There is indication that the largest effect can be found during summer.
- It is shown that the assimilation of sea-ice concentration is particularly beneficial for predictions along the sea-ice edge while sea-ice thickness is more important for the central Arctic. Hence, the assimilation of both is complementary and yields the best overall result. The assimilation of C2SMOS data provides significantly better results compared to ENVISAT CCI.
- Assimilation of Arctic data to produce initial fields should be carried out typically at least a few decades to robustly test the impact on prediction quality.
- Arctic river runoff predictions for regional and/or pan-Arctic applications can be improved by assimilation of observational data, but the access to provisional data need to be improved for real-time analyses.

Exploitation

Stakeholders of this task, 6.1, include the climate prediction community, climate services such as the European Copernicus Climate Services (C3S) and the respective users in various societal and economic sectors. For the benefits of stakeholders, results from the task can be and should be further exploited.

The output of this task includes improved ways of prediction skill assessment and improved predictions, whereby the improvement relates to the availability of observational data, or data that is derived from observations. These results should be further exploited after the end of the project by climate prediction groups. From the recommendations above it appears obvious that

- Sea-ice concentrations and sea-ice thickness together should be assimilated routinely into the assimilation procedures that generate initialization conditions for the respective climate model. Updates of those observations data should be utilized as soon as available. Thereby, also improvements of past observations, decades back, would have a positive effect on the initial fields.
- A more general way of exploiting sea-ice data is the inclusion into major reanalysis products by ECMWF, which are easily accessible by numerous climate modelling and prediction groups.
- Runoff data were available should be routinely used for reanalysis products. Those in turn could be used for improved runoff predictions providing river discharge to the climate prediction community and forecast products for local and regional stakeholder.

Roadmap

A roadmap towards a sustainable iAOS with a benefit for climate prediction needs to ensure continuous access to sea-ice concentration and thickness data, for forthcoming new observations and backwards in times. Data need to be ready as input to assimilation into prediction and reanalysis systems. Here we demonstrated accessibility and usefulness for climate prediction models. Again, it is worth to note that availability of the observations data for standard re-analysis products at ECMWF is essential because these products are strongly used by the climate prediction communities.

A roadmap for a sustainable river discharge observation system should be based on (1) user requirements ranging from pan-Arctic climate and ocean modelling to regional and local flood forecasting (2) strengths and weaknesses of the traditional in-situ observation networks (assessed in WP2) (3) the potential of existing and future satellite missions and remote sensing, and (4) the capacity of hydrological model and data assimilation to integrate in-situ and remote sensing data to fill the temporal and spatial gaps. The in-situ based river discharge data provided by national hydrological services will be the basis also in a future monitoring system but need to be improved primarily in terms of accessibility and interoperability.

Observations of river water level by satellite altimetry and subsequent transformation to river discharge will also be a very important contribution to a future monitoring system, which will extend the spatial coverage of the current observation system and potentially increase access to observations in near real time. However, these methodologies and data were not part of INTAROS. Even with increased spatial coverage by satellite data, the hydrological model will

be a necessary ingredient to fill the temporal and spatial gaps in the available observations to obtain a sustainable and reliable river discharge monitoring system.

References

Acosta Navarro, J.C., Ortega, P., Batté, L., Smith, D., Bretonnière, P.A., Guemas, V., Massonnet, F., Sicardi, V., Torralba, V., Tourigny, E. and Doblas-Reyes, F.J., 2020. Link between autumnal Arctic sea-ice and Northern Hemisphere winter forecast skill. Geophysical Research Letters, 47(5), p.e2019GL086753.

Arheimer B. et al. (2020) Global catchment modelling using World-Wide HYPE (WWH), open data, and stepwise parameter estimation, Hydrol. Earth Syst. Sci., 24, 535–559, https://doi.org/10.5194/hess-24-535-2020

Berg, P., Donnelly, C., and Gustafsson, D. (2018). Near-real-time adjusted reanalysis forcing data for hydrology, Hydrol. Earth Syst. Sci., 22, 989–1000, https://doi.org/10.5194/hess-22-989-2018.

Bethke, I., Wang, Y., Counillon, F., Keenlyside, N., Kimmritz, M., Fransner, F., Samuelsen, A., Langehaug, H., Svendsen, L., Chiu, P.G. and Passos, L., 2021. NorCPM1 and its contribution to CMIP6 DCPP. Geoscientific Model Development Discussions, pp.1-84.

Bushuk, M. and Giannakis, D., 2017. The seasonality and interannual variability of Arctic sea-ice reemergence. Journal of Climate, 30(12), pp.4657-4676.

Counillon, F., Bethke, I., Keenlyside, N., Bentsen, M., Bertino, L., & Zheng, F. (2014). Seasonal-to-decadal predictions with the ensemble Kalman filter and the Norwegian Earth System Model: a twin experiment. Tellus A, 66. doi:10.3402/tellusa.v66.21074

Counillon F, Keenlyside N, Bethke I, Wang Y, Billeau S, Shen M-L, et al. Flow-dependent assimilation of sea surface temperature in isopycnal coordinates with the Norwegian climate prediction model. Tellus. Series A, Dynamic meteorology and oceanography. 2016;68:32437.

Dai P, Gao Y, Counillon F, Wang Y, Kimmritz M, Langehaug HR. Seasonal to decadal predictions of regional Arctic sea-ice by assimilating sea surface temperature in the Norwegian Climate Prediction Model. Climate Dynamics. 2020

Döscher, R., Acosta, M., Alessandri, A., Anthoni, P., Arneth, A., Arsouze, T., Bergmann, T., Bernadello, R., Bousetta, S., Caron, L.-P., Carver, G., Castrillo, M., Catalano, F., Cvijanovic, I., Davini, P., Dekker, E., Doblas-Reyes, F. J., Docquier, D., Echevarria, P., Fladrich, U., Fuentes-Franco, R., Gröger, M., v. Hardenberg, J., Hieronymus, J., Karami, M. P., Keskinen, J.-P., Koenigk, T., Makkonen, R., Massonnet, F., Ménégoz, M., Miller, P. A., Moreno-Chamarro, E., Nieradzik, L., van Noije, T., Nolan, P., O'Donnell, D., Ollinaho, P., van den Oord, G., Ortega, P., Prims, O. T., Ramos, A., Reerink, T., Rousset, C., Ruprich-Robert, Y., Le Sager, P., Schmith, T., Schrödner, R., Serva, F., Sicardi, V., Sloth Madsen, M., Smith, B., Tian, T., Tourigny, E., Uotila, P., Vancoppenolle, M., Wang, S., Wårlind, D., Willén, U., Wyser, K., Yang, S., Yepes-Arbós, X., and Zhang, Q.: The EC-Earth3 Earth System Model for the Climate Model Intercomparison Project 6, *Geosci. Model Dev. Discuss.* [preprint], https://doi.org/10.5194/gmd-2020-446, accepted for publication in Geosci. Model Dev., 2021.

Gelfan A. et al. (2017) Climate change impact on the water regime of two great Arctic rivers: modeling and uncertainty issues. Climatic Change,141 (3): 499-515. doi:10.1007/s10584-016-1710-5. Number of citations: 42.

Girard-Ardhuin, F., and Piollé, J.-F. "Ifremer/CERSAT long-term sea ice satellite datasets." AGU Fall Meeting Abstracts. Vol. 2018. 2018.

Hendricks, S.; Paul, S.; Rinne, E. (2018): ESA Sea Ice Climate Change Initiative (Sea_Ice_cci): Northern hemisphere sea ice thickness from the CryoSat-2 satellite on a monthly grid (L3C), v2.0. Centre for Environmental Data Analysis, date of citation. doi:10.5285/ff79d140824f42dd92b204b4f1e9e7c2.

Hersbach, H.; Bell, B.; Berrisford, P.; Hirahara, S.; Horanyi, A.; Munoz-Sabater, J.; Nicolas, J.; Peubey, C.; Radu, R.; Schepers, D.; Simmons, A.; Soci, C.; Abdalla, S.; Abellan, X.; Balsamo, G.; Bechtold, P.; Biavati, G.; Bidlot, J.; Bonavita, M.; De Chiara, G.; Dahlgren, P.; Dee, D.; Diamantakis, M.; Dragani, R.; Flemming, J.; Forbes, R.; Fuentes, M.; Geer, A.; Haimberger, L.; Healy, S.; Hogan, R. J.; Holm, E.; Janiskova, M.; Keeley, S.; Laloyaux, P.; Lopez, P.; Lupu, C.; Radnoti, G.; de Rosnay, P.; Rozum, I.; Vamborg, F.; Villaume, S. & Thepaut, J. N.: The ERA5 global reanalysis. *Quarterly Journal of the Royal Meteorological Society*, 146, 1999-2049, 2020

Karami, M.P., T. Kruschke, T. Tian, T. Koenigk, S. Yang, F. Schenk: Prediction skill in decadal climate simulations of the EC-Earth3 model with a focus on the Arctic sea ice. In preparation.

Kimmritz, M., Counillon, F., Smedsrud, L. H., Bethke, I., Keenlyside, N., Ogawa, F., & Wang, Y. (2019). Impact of ocean and sea ice initialisation on seasonal prediction skill in the Arctic. Journal of Advances in Modeling Earth Systems, 11.

Lavergne, T., Sørensen, A.M., Kern, S., Tonboe, R., Notz, D., Aaboe, S., Bell, L., Dybkjær, G., Eastwood, S., Gabarro, C. and Heygster, G., 2019. Version 2 of the EUMETSAT OSI SAF and ESA CCI sea-ice concentration climate data records. The Cryosphere, 13(1), pp.49-78.

Lindström G. et al (2010). Development and test of the HYPE (Hydrological Predictions for the Environment) model – A water quality model for different spatial scales. Hydrology Research 41.3-4:295-319.

MacDonald M. K. et al. (2018). Impacts of 1.5 and 2.0 °C warming on pan-Arctic river discharge into the Hudson Bay Complex through 2070. Geophysical Research Letters, 45, 7561–7570. https://doi.org/10.1029/2018GL079147. Number of citations: 7.

Ricker, R., Hendricks, S., Kaleschke, L., Tian-Kunze, X., King, J., and Haas, C.: A weekly Arctic sea-ice thickness data record from merged CryoSat-2 and SMOS satellite data, The Cryosphere, 11, 1607–1623, https://doi.org/10.5194/tc-11-1607-2017, 2017.

Sakov, P., Counillon, F., Bertino, L., Lisæter, K.A., Oke, P.R. and Korablev, A., 2012. TOPAZ4: an ocean-sea-ice data assimilation system for the North Atlantic and Arctic. Ocean Science, 8(4), pp.633-656.

SMHI Hydrological Research and Development: HYPEweb (www.hypeweb.smhi.se), giving access to some HYPE model results, HYPE model code and other water services.

Tian, T., Yang, S., Karami, M. P., Massonnet, F., Kruschke, T., and Koenigk, T.: Benefits of sea-ice initialization for the interannual-to-decadal climate prediction skill in the Arctic in

EC-Earth3, *Geosci. Model Dev.*, 14, 4283–4305, https://doi.org/10.5194/gmd-14-4283-2021, 2021.

Wang, Y., Counillon, F., Keenlyside, N. et al. Seasonal predictions initialised by assimilating sea surface temperature observations with the EnKF, Clim Dyn, 2019. https://doi.org/10.1007/s00382-019-04897-9

Wingham, D. J., Francis, C. R., Baker, S., Bouzinac, C., Brockley, D., Cullen, R., ... & Wallis, D. W. (2006). CryoSat: A mission to determine the fluctuations in Earth's land and marine ice fields. *Advances in Space Research*, *37*(4), 841-871.

Xie, J., Counillon, F. and Bertino, L., 2018. Impact of assimilating a merged sea-ice thickness from CryoSat-2 and SMOS in the Arctic reanalysis. The Cryosphere, 12(11), pp.3671-3691.

Zuo, H., Balmaseda, M.A., Tietsche, S., Mogensen, K. and Mayer, M., 2019. The ECMWF operational ensemble reanalysis–analysis system for ocean and sea-ice: a description of the system and assessment. Ocean science, 15(3), pp.779-808.

Årthun, M., R. C. J. Wills, H. L. Johnson, L. Chafik and H. R. Langehaug (2021). "Mechanisms of decadal North Atlantic climate variability and implications for the recent cold anomaly." Journal of Climate: 1-52, 34(9), 3421-3439)

--- END OF DOCUMENT ---

INTAROS

This report is made under the project
Integrated Arctic Observation System (INTAROS)
funded by the European Commission Horizon 2020 program
Grant Agreement no. 727890.

Project partners: